

# Sampling Method for Generalized Graph Signals with Pre-selected Vertices via DC Optimization

Keitaro Yamashita<sup>1</sup>, Student Member, IEEE, Kazuki Naganuma<sup>2</sup>, Member, IEEE, and Shunsuke Ono<sup>1</sup>, Senior Member, IEEE

<sup>1</sup>Institute of Science Tokyo, Tokyo, Japan

<sup>2</sup>Tokyo University of Agriculture and Technology, Tokyo, Japan

Corresponding author: Keitaro Yamashita (email: yamashita.k.45d1@m.isct.ac.jp).

This work was supported in part by JST FOREST under Grant JPMJFR232M, JST AdCORP under Grant JPMJKB2307, JST ACT-X Grant under JPMJAX23CJ, JSPS KAKENHI under Grant 22H03610, 22H00512, 23H01415, 23K17461, 24K03119, 24K22291, 25H01296, and 25K03136, and Grant-in-Aid for JSPS Fellows under 25KJ0117.

## ABSTRACT

This paper proposes a method for vertex-wise flexible sampling of a broad class of graph signals, designed to attain the best possible recovery based on the generalized sampling theory. This is achieved by designing a sampling operator by an optimization problem, which is inherently non-convex, as the best possible recovery imposes a rank constraint. An existing method for vertex-wise flexible sampling is able to control the number of active vertices but cannot incorporate prior knowledge of mandatory or forbidden vertices. To address these challenges, we formulate the operator design as a problem that handles a constraint of the number of active vertices and prior knowledge on specific vertices for sampling, mandatory inclusion or exclusion. We transformed this constrained problem into a difference-of-convex (DC) optimization problem by using the nuclear norm and a DC penalty for vertex selection. To solve this, we develop a convergent solver based on the general double-proximal gradient DC algorithm. The effectiveness of our method is demonstrated through experiments on various graph signal models, including real-world data, showing superior performance in the recovery accuracy by comparing to existing methods.

**INDEX TERMS** difference-of-convex optimization, generalized sampling theory, graph signal processing, graph signal sampling, vertex-wise flexible sampling.

## I. INTRODUCTION

Graph signal processing (GSP) has emerged as a powerful framework for analyzing data on irregular structures, extending classical signal processing theories to the graph setting [1]–[4]. This paradigm has proven invaluable in numerous fields by providing tools to handle complex and diverse data. Various research topics are associated with GSP, including graph learning [5]–[7], graph restoration and signal recovery [8]–[12]. Its applications span various domains, such as social network analysis, brain network studies, transportation modeling, image analysis, artificial intelligence, and wireless sensor systems [13]–[16].

A key aspect of GSP is graph signal sampling. Sampling enables efficient data storage and transmission by reducing dimension of data and can reduce costs and energy consump-

tion by limiting the number of active sensors in physical networks [17]. Unlike its classical counterpart in time-series signal processing, graph signal sampling is more challenging as it lacks a regular, shift-invariant structure [17], [18]. Initial research focused on extending the Shannon-Nyquist theorem to the graph domain, leading to sampling bandlimited graph signals [18]–[26]. However, the bandlimited assumption is often too restrictive for applications with localized features or sharp transitions, such as meteorological data in mountainous areas, landscape image data, and water distribution network data [5], [13], [27].

To address this limitation, the *generalized sampling theory* [28], [29] has been extended to the graph domain. This theory provides a unified framework for achieving the best possible recovery of beyond bandlimited signals based on

signal priors. This extension enables to handle sampling beyond bandlimited graph signals [4], [17], [23], [30]–[37].

Within the generalized sampling framework, a key challenge is to design a sampling operator that ensures high-precision recovery for beyond bandlimited graph signals with keeping the benefits of sampling, such as data compression and sensor reduction. Early methods focused on two main strategies: *vertex-wise sampling*, which selects a subset of vertices [33], and *flexible sampling*, which forms samples from a linear combination of all vertices [32], [35], [36]. While vertex-wise sampling is efficient, it can be sensitive to noise as its high dependence on the selected vertices. Flexible sampling offers greater robustness but requires data from all vertices, negating the benefit of sensor reduction. To balance these trade-offs, *vertex-wise flexible sampling* was introduced, controlling the number of sample-contributive vertices [37]. This approach achieves the robustness of flexible sampling while using data from limited vertices.

Despite these advances, a significant practical research gap remains. While existing vertex-wise flexible sampling methods can control the quantity of active vertices, they cannot handle prior knowledge about specific vertices whether they should or should not be used. This limitation is critical in many real-world applications. For instance, in a sensor network, certain sensors may be mandatory due to their high demands or strategic location, while others may be forbidden due to high operational costs or physical unavailability. Furthermore, the method in [37] designs a sampling operator with a non-convex optimization problem that its algorithm is not theoretically guaranteed to be convergent. This lack of a convergence guarantee can lead to an unstable sampling operator design.

These limitations lead to the following research question: *How can we design a sampling operator for vertex-wise flexible sampling that achieves the best possible recovery, allows us to control the number of sample-contributive vertices with prior knowledge of mandatory and forbidden vertices, and is based on a convergent algorithm?*

Our main contributions to address this question are:

- Formulate a sampling operator design problem that allows for the pre-selection of two distinct vertex sets (sets of sample-contributive vertices and non sample-contributive vertices) while controlling the total number of sample-contributive vertices.
- Reformulate this constrained problem into a difference-of-convex (DC) optimization problem<sup>1</sup> with tightly relaxing the constraint to achieve the best possible recovery and the constraint to control the number of sample-contributive vertices as a DC penalty.
- Develop a solver based on the general double-proximal gradient DC (GDPGDC) algorithm, which guarantees its convergence to a critical point of the proposed problem.

<sup>1</sup>DC optimization has recently been used in signal processing [38], [39].

TABLE 1. Notations and Definitions.

Notations	Definitions
$\mathcal{X}$	a set
$\mathbf{x}$	a vector
$x_i, [\mathbf{x}]_{ij}$	the $i$ -th element of $\mathbf{x}$
$\ \mathbf{x}\ _2$	the $\ell_2$ norm of $\mathbf{x}$ , $\ \mathbf{x}\ _2 := \sqrt{\sum_i x_i^2}$
$\mathbf{X}$	a matrix
$\mathbf{x}_{(i)}, [\mathbf{X}]_{(i)}$	the $i$ -th row vector of $\mathbf{X}$
$X_{ij}, [\mathbf{X}]_{ij}$	the $(i, j)$ -th element of $\mathbf{X}$
$\mathbf{X}^\top$	the transpose of $\mathbf{X}$
$\mathbf{X}^{-1}$	the inverse of $\mathbf{X}$
$\mathbf{X}^\dagger$	the pseudo-inverse of $\mathbf{X}$
$\sigma_i(\mathbf{X})$	the $i$ -th singular value of $\mathbf{X}$
$\ \mathbf{X}\ _F$	the Frobenius norm of $\mathbf{X}$ , $\ \mathbf{X}\ _F := \sqrt{\langle \mathbf{X}, \mathbf{X} \rangle}$
$\ \mathbf{X}\ _*$	the nuclear norm of $\mathbf{X}$ , $\ \mathbf{X}\ _* := \sum_i \sigma_i(\mathbf{X})$
$\iota_{\mathcal{C}}(\mathbf{X})$	the indicator function of a closed set $\mathcal{C}$ , $\iota_{\mathcal{C}}(\mathbf{X}) = \begin{cases} 0 & \text{if } \mathbf{X} \in \mathcal{C} \\ \infty & \text{otherwise} \end{cases}$
$\mathbf{0}$	a zero vector

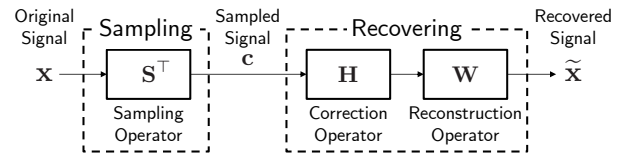


FIGURE 1. Generalized sampling framework for graph signals.

This paper is organized as follows. Section II reviews the fundamentals of graph signal sampling and the GDPGDC algorithm. Section III details the proposed method. Section IV presents experimental results to demonstrate its effectiveness. Section V concludes the paper.

## II. PRELIMINARIES

This section establishes the background of our proposed method. We review the principles of generalized sampling for the graph domain. Then, we introduce the GDPGDC algorithm, which is the optimization tool to solve our proposed problem. A list of notations is provided in Table 1.

### A. Generalized Sampling of Graph Signals

Here, we provide a concise overview of the generalized sampling framework for graph signals [4], [17], [29], which forms the foundation of our approach. We consider a weighted, undirected graph with  $N$  vertices.

The overall process of sampling and recovery is illustrated in Fig. 1. An original graph signal, denoted by  $\mathbf{x} \in \mathcal{X} \subseteq \mathbb{R}^N$ , is transformed into a sampled signal  $\mathbf{c} \in \mathbb{R}^M$  (where  $M \leq N$ ) by a sampling operator  $\mathbf{S}^\top \in \mathbb{R}^{M \times N}$ . Thus, the sampled signal is defined as  $\mathbf{c} := \mathbf{S}^\top \mathbf{x}$ . To recover the signal, the sampled signal  $\mathbf{c}$  is first processed by a correction operator  $\mathbf{H}$  and then mapped back to the graph by a reconstruction operator  $\mathbf{W}$ . The final recovered signal  $\tilde{\mathbf{x}} \in \mathcal{X}$  is given by

$$\tilde{\mathbf{x}} = \mathbf{W}\mathbf{H}\mathbf{c} = \mathbf{W}\mathbf{H}\mathbf{S}^\top \mathbf{x}. \quad (1)$$

The reconstruction operator  $\mathbf{W}$  can be fixed due to computational or hardware constraints. In this paper, we focus on the unconstrained case for simplicity.

The optimal operators  $\mathbf{H}$  and  $\mathbf{W}$  can be designed with assuming prior knowledge about the signal priors. In what follows, we provide an overview of the signal priors and the corresponding design of  $\mathbf{H}$  and  $\mathbf{W}$  in the generalized sampling theory, drawing from prior works [4], [34].

### 1) Subspace prior

Under the subspace prior, we suppose that a graph signal  $\mathbf{x} \in \mathbb{R}^N$  is characterized by a linear model as follows:

$$\mathbf{x} := \mathbf{A}\mathbf{d}, \quad (2)$$

where  $\mathbf{A} \in \mathbb{R}^{N \times K}$  ( $K \leq N$ ) is a known generator matrix and  $\mathbf{d} \in \mathbb{R}^K$  is an expansion coefficient vector. Under this prior, with a given  $\mathbf{S}$ , it is known that  $\tilde{\mathbf{x}}$  is given as follows:

$$\tilde{\mathbf{x}} = \mathbf{A}(\mathbf{S}^\top \mathbf{A})^\dagger \mathbf{S}^\top \mathbf{x}. \quad (3)$$

Then, the operators  $\mathbf{H}$  and  $\mathbf{W}$  are given by

$$\mathbf{H} = (\mathbf{S}^\top \mathbf{A})^\dagger, \quad \mathbf{W} = \mathbf{A}. \quad (4)$$

### 2) Smoothness prior

Under the smoothness prior, the signal  $\mathbf{x}$  is assumed to be smooth as:  $\|\mathbf{F}\mathbf{x}\|_2^2 \leq \rho^2$  for some constant  $\rho$ , where  $\mathbf{F} \in \mathbb{R}^{N \times N}$  is the invertible operator that quantifies the variation of  $\mathbf{x}$ . Under this prior, with a given  $\mathbf{S}$ , it is known that  $\tilde{\mathbf{x}}$  is given as follows:

$$\tilde{\mathbf{x}} = \widetilde{\mathbf{W}}(\mathbf{S}^\top \widetilde{\mathbf{W}})^\dagger \mathbf{S}^\top \mathbf{x}, \quad (5)$$

where  $\widetilde{\mathbf{W}} = (\mathbf{F}^\top \mathbf{F})^{-1} \mathbf{S}$ . Then, the operators  $\mathbf{H}$  and  $\mathbf{W}$  are given by

$$\mathbf{H} = (\mathbf{S}^\top \widetilde{\mathbf{W}})^\dagger, \quad \mathbf{W} = \widetilde{\mathbf{W}} = (\mathbf{F}^\top \mathbf{F})^{-1} \mathbf{S}. \quad (6)$$

### 3) Stochastic prior

Under the stochastic prior, we consider that the samples can be obtained with an additive noise  $\boldsymbol{\eta} \in \mathbb{R}^M$  and recover from the noisy sample signal  $\mathbf{y} = \mathbf{c} + \boldsymbol{\eta}$  as follows:

$$\tilde{\mathbf{x}} = \mathbf{W}\mathbf{H}\mathbf{y} = \mathbf{W}\mathbf{H}(\mathbf{c} + \boldsymbol{\eta}) = \mathbf{W}\mathbf{H}(\mathbf{S}^\top \mathbf{x} + \boldsymbol{\eta}). \quad (7)$$

Suppose a graph signal  $\mathbf{x}$  as a zero-mean process characterized by graph wide sense stationarity (GWSS) [34]. The graph signal  $\mathbf{x}$  and the noise  $\boldsymbol{\eta}$  is associated with a known covariance matrix  $\boldsymbol{\Gamma}_{\mathbf{x}} \in \mathbb{R}^{N \times N}$  and  $\boldsymbol{\Gamma}_{\boldsymbol{\eta}} \in \mathbb{R}^{M \times M}$ , respectively. Both  $\boldsymbol{\Gamma}_{\mathbf{x}}$  and  $\boldsymbol{\Gamma}_{\boldsymbol{\eta}}$  are autocorrelation matrices. Under this prior, with a given  $\mathbf{S}$ , it is known that  $\tilde{\mathbf{x}}$  is given as follows:

$$\tilde{\mathbf{x}} = \boldsymbol{\Gamma}_{\mathbf{x}} \mathbf{S} (\mathbf{S}^\top \boldsymbol{\Gamma}_{\mathbf{x}} \mathbf{S} + \boldsymbol{\Gamma}_{\boldsymbol{\eta}})^\dagger (\mathbf{S}^\top \mathbf{x} + \boldsymbol{\eta}). \quad (8)$$

Then, the operators  $\mathbf{H}$  and  $\mathbf{W}$  are given by

$$\mathbf{H} = (\mathbf{S}^\top \boldsymbol{\Gamma}_{\mathbf{x}} \mathbf{S} + \boldsymbol{\Gamma}_{\boldsymbol{\eta}})^\dagger, \quad \mathbf{W} = \boldsymbol{\Gamma}_{\mathbf{x}} \mathbf{S}. \quad (9)$$

## B. General Double-Proximal Gradient DC Algorithm

This subsection details the *general double-proximal gradient DC* (GDPGDC) algorithm [40], a versatile and conver-

gent method for solving optimization problems involving a difference-of-convex (DC) structure. The GDPGDC algorithm is designed to address problems of the form

$$\min_{\mathbf{X}} f_1(\mathbf{X}) + f_2(\mathbf{X}) - h(\mathbf{B}\mathbf{X}), \quad (10)$$

where  $f_1 : \mathbb{R}^{n \times m} \rightarrow \mathbb{R}$  is a differentiable convex function with a  $1/\beta$ -Lipschitz continuous gradient for some  $\beta > 0$ ,  $f_2 : \mathbb{R}^{n \times m} \rightarrow \overline{\mathbb{R}}$  and  $h : \mathbb{R}^{k \times m} \rightarrow \overline{\mathbb{R}}$  are proper, lower-semicontinuous, convex functions, with  $\overline{\mathbb{R}} := \mathbb{R} \cup \{\infty\}$ , and  $\mathbf{B} : \mathbb{R}^{k \times n}$  is a linear operator.

The GDPGDC algorithm solves Prob. (10) through an iterative process. Given step-size parameters  $\gamma_1, \gamma_2 > 0$  and starting from an initial point  $(\mathbf{X}^{(0)}, \mathbf{Z}^{(0)})$ , the algorithm proceeds by alternating between updates for the primal variable  $\mathbf{X}$  and a dual variable  $\mathbf{Z}$ :

$$\begin{cases} \mathbf{X}^{(t+1)} \leftarrow \text{prox}_{\gamma_1 f_2}(\mathbf{X}^{(t)} - \gamma_1 (\nabla f_1(\mathbf{X}^{(t)}) - \mathbf{B}^\top \mathbf{Z}^{(t)})); \\ \mathbf{Z}^{(t+1)} \leftarrow \text{prox}_{\gamma_2 h^*}(\mathbf{Z}^{(t)} + \gamma_2 \mathbf{B}\mathbf{X}^{(t+1)}); \\ t \leftarrow t + 1. \end{cases} \quad (11)$$

Here, the proximity operator  $\text{prox}_{\gamma f}(\cdot)$  for a proper, lower-semicontinuous, convex function  $f$  and a parameter  $\gamma > 0$  is defined as

$$\text{prox}_{\gamma f}(\mathbf{X}) := \underset{\mathbf{Y}}{\text{argmin}} \left\{ f(\mathbf{Y}) + \frac{1}{2\gamma} \|\mathbf{X} - \mathbf{Y}\|_F^2 \right\}. \quad (12)$$

The update for  $\mathbf{Z}$  involves the proximity operator of  $h^*$ , the *Fenchel–Rockafellar conjugate function*<sup>2</sup> of  $h$ . This can be computed by using Moreau's identity [41, Theorem 14.3(ii)] as

$$\text{prox}_{\gamma h^*}(\mathbf{X}) = \mathbf{X} - \gamma \text{prox}_{\frac{1}{\gamma} h} \left( \frac{1}{\gamma} \mathbf{X} \right). \quad (13)$$

The convergence properties of this algorithm are well-established. The following theorem provides the conditions under which the sequence generated by the GDPGDC algorithm converges to a critical point.

**Theorem 1** ([40, Proposition 4] Convergence of GDPGDC). *Assume that the objective function in Prob. (10) is bounded from below. Let the step-sizes satisfy  $0 < \gamma_1^{(t)} < 2\beta$  and  $0 < \gamma_2^{(t)} < +\infty$ . If the sequences  $\{\mathbf{X}^{(t)}\}_{t \in \mathbb{N}}$  and  $\{\mathbf{Z}^{(t)}\}_{t \in \mathbb{N}}$  generated by the iterative scheme (11) are bounded, then any cluster point of  $\{\mathbf{X}^{(t)}\}_{t \in \mathbb{N}}$  is a critical point of Prob. (10).*

## III. Proposed Method

In this section, we present our method for designing a sampling operator,  $\mathbf{S}$ . As established in Sec. II, the recovery process in Eq. (1) relies on a correction operator  $\mathbf{H}$  and a reconstruction operator  $\mathbf{W}$ , which are designed for each signal prior as summarized in Table 2. Our primary goal is to design a  $\mathbf{S}$  that is appropriate for the process with accommodating prior knowledge about which vertices must or must not contribute to the sampling.

<sup>2</sup>The *Fenchel–Rockafellar conjugate function* of  $h$  is defined as  $h^*(\mathbf{X}) := \max_{\mathbf{Y}} \langle \mathbf{X}, \mathbf{Y} \rangle - h(\mathbf{Y})$ , where  $\langle \mathbf{X}, \mathbf{Y} \rangle$  denotes the inner product of  $\mathbf{X}$  and  $\mathbf{Y}$ ,  $\langle \mathbf{X}, \mathbf{Y} \rangle := \sum_i \sum_j X_{ij} Y_{ij}$ .

**TABLE 2. Designs of the Collection Operator  $\mathbf{H}$ , the Reconstruction Operator  $\mathbf{W}$ , and the Matrix  $\mathbf{P}$ . The Following Definitions Are Used:  $\widetilde{\mathbf{W}} = (\mathbf{F}^\top \mathbf{F})^{-1} \mathbf{S}$ ,  $\mathbf{F} = \mathbf{U}_F \Sigma_F \mathbf{V}_F^\top$ , and  $\Gamma_x = \mathbf{Q}^\top \mathbf{Q}$ .**

Prior	$\mathbf{H}$	$\mathbf{W}$	$\mathbf{P}$
Subspace	$(\mathbf{S}^\top \mathbf{A})^\dagger$	$\mathbf{A}$	$\mathbf{A}^\top$
Smoothness	$(\mathbf{S}^\top \widetilde{\mathbf{W}})^\dagger$	$\widetilde{\mathbf{W}}$	$\Sigma_F^{-1} \mathbf{V}_F^\top$
Stochastic	$(\mathbf{S}^\top \Gamma_x \mathbf{S} + \Gamma_\eta)^\dagger$	$\Gamma_x \mathbf{S}$	$\mathbf{Q}$

### A. The Condition for Designing the Sampling Operator

In this subsection, we discuss about the condition for designing a sampling operator on each prior by using the solutions about recovered signals introduced in subsection A before discussing the specific designing method for the sampling operator. In order to achieve the best possible recovery based on Eqs. (1) and (7), we try to find  $\mathbf{S}$  ensuring that the correction operator  $\mathbf{H}$  has the full rank. To account for the differences in the designs of  $\mathbf{H}$  for each signal prior, we introduce a matrix  $\mathbf{P}$  to find an appropriate  $\mathbf{S}$  that satisfies the condition that  $\mathbf{H}$  has the full rank. This matrix  $\mathbf{P}$  is derived based on the conditions of each signal prior, as summarized in Table 2. We will now examine the conditions of  $\mathbf{P}$  on a prior-by-prior basis, and it should be noted that we seek  $\mathbf{S}$  such that  $(\mathbf{P}\mathbf{S})^\top \mathbf{P}\mathbf{S}$  is invertible as a result.

#### 1) Subspace Prior

Based on (3), we seek  $\mathbf{S}$  for which  $(\mathbf{S}^\top \mathbf{A})^\dagger$  has the full column rank, i.e.,  $\mathbf{S}^\top \mathbf{A}$  has the full row rank. Thus, we need to find  $\mathbf{S}$  such that  $\mathbf{S}^\top \mathbf{A} (\mathbf{S}^\top \mathbf{A})^\top$  is invertible, i.e.  $(\mathbf{A}^\top \mathbf{S})^\top \mathbf{A}^\top \mathbf{S}$  is invertible. Thus, the matrix  $\mathbf{P}$  results as

$$\mathbf{P} = \mathbf{A}^\top. \quad (14)$$

#### 2) Smoothness Prior

Based on (5), for the unconstrained case, we seek  $\mathbf{S}$  for which  $(\mathbf{S}^\top \widetilde{\mathbf{W}})^\dagger = (\mathbf{S}^\top \widetilde{\mathbf{W}})^{-1}$ , i.e.,  $\mathbf{S}^\top \widetilde{\mathbf{W}}$  is invertible. Let us define the singular value decomposition (SVD) of  $\mathbf{F}$  as  $\mathbf{F} = \mathbf{U}_F \Sigma_F \mathbf{V}_F^\top$ . Then,  $\mathbf{S}^\top \widetilde{\mathbf{W}}$  is transformed as follows:

$$\begin{aligned} \mathbf{S}^\top \widetilde{\mathbf{W}} &= \mathbf{S}^\top (\mathbf{F}^\top \mathbf{F})^{-1} \mathbf{S} \\ &= \mathbf{S}^\top (\mathbf{V}_F \Sigma_F^2 \mathbf{V}_F^\top)^{-1} \mathbf{S} \\ &= (\Sigma_F^{-1} \mathbf{V}_F^\top \mathbf{S})^\top \Sigma_F^{-1} \mathbf{V}_F^\top \mathbf{S}. \end{aligned} \quad (15)$$

Consequently, one can see that  $\mathbf{S}^\top \widetilde{\mathbf{W}}$  is invertible if and only if  $\Sigma_F^{-1} \mathbf{V}_F^\top \mathbf{S} \in \mathbb{R}^{N \times M}$  has the full column rank so that the matrix  $\mathbf{P}$  results as

$$\mathbf{P} = \Sigma_F^{-1} \mathbf{V}_F^\top. \quad (16)$$

#### 3) Stochastic Prior

Based on (8), we seek  $\mathbf{S}$  for which  $(\mathbf{S}^\top \Gamma_x \mathbf{S} + \Gamma_\eta)^\dagger = (\mathbf{S}^\top \Gamma_x \mathbf{S} + \Gamma_\eta)^{-1}$ , i.e.,  $\mathbf{S}^\top \Gamma_x \mathbf{S} + \Gamma_\eta$  is invertible. Due to the characteristics of an autocorrelation matrix,  $\mathbf{S}^\top \Gamma_x \mathbf{S} + \Gamma_\eta$  is invertible if  $\mathbf{S}^\top \Gamma_x \mathbf{S}$  is invertible. Since  $\Gamma_x$  is symmetric, for some  $\mathbf{Q} \in \mathbb{R}^{N \times N}$ ,  $\Gamma_x$  can be decomposed as  $\Gamma_x = \mathbf{Q}^\top \mathbf{Q}$ .

Then  $\mathbf{S}^\top \Gamma_x \mathbf{S} = (\mathbf{Q}\mathbf{S})^\top \mathbf{Q}\mathbf{S}$  is invertible if and only if  $\mathbf{Q}\mathbf{S} \in \mathbb{R}^{N \times M}$  has the full column rank. Therefore, the matrix

$\mathbf{P}$  results as

$$\mathbf{P} = \mathbf{Q}. \quad (17)$$

### B. Problem Formulation

To incorporate such prior knowledge about the vertices, we partition the set of all vertices  $\mathcal{V}$  into three disjoint sets: the set of vertices that are known to be sample-contributive,  $\mathcal{V}_C$ ; the set of vertices that are known to be non-sample-contributive,  $\mathcal{V}_K$ ; and the set of vertices for which it is unknown whether they are to be sample-contributive,  $\mathcal{V}_U$ . We also define  $L$  ( $L \leq N$ ) as the desired upper limit on the total number of sample-contributive vertices. From this, the upper limit on the number of sample-contributive vertices to be selected from the undecided set  $\mathcal{V}_U$  is denoted by  $L' = L - |\mathcal{V}_C|$ .

To achieve the best possible signal recovery,  $\mathbf{S}$  should satisfy the ideal conditions derived from the generalized sampling theory; in particular,  $\mathbf{P}\mathbf{S}$  has full rank. Additionally, we must enforce the structural constraints on  $\mathbf{S}$  based on our vertex partitioning.

First, we formulate our ideal conditions as a feasibility problem as follows, which seeks a sampling operator  $\mathbf{S}$  that satisfies all desired constraints simultaneously:

$$\text{find } \mathbf{S} \quad \text{s.t.} \quad \begin{cases} \mathbf{S} \in \mathcal{C}_{\mathcal{V}_K}, \\ \mathbf{S} \in \mathcal{C}_{L'}, \\ \text{rank}(\mathbf{P}\mathbf{S}) = R, \end{cases} \quad (18)$$

where  $\mathcal{C}_{\mathcal{V}_K} := \{\mathbf{X} \mid \mathbf{x}_{(i)} = \mathbf{0}, \forall i \in \mathcal{V}_K\}$  is the set of matrices respecting the non-contributive constraint,  $\mathcal{C}_{L'} := \{\mathbf{X} \mid |\{i \in \mathcal{V}_U \mid \|\mathbf{x}_{(i)}\|_2 \neq 0\}| \leq L'\}$  restricts the number of contributing vertices from the undecided set, and  $R$  is the largest possible rank of  $\mathbf{P}\mathbf{S}$ .

However, the rank constraint and the combinatorial vertex selection constraint in (18) are intractable to handle directly. As the first step, we relax the hard rank constraint into the tightest convex approximation of the rank function that we use the nuclear norm and reframe the problem as a constrained maximization by following [42]:

$$\max_{\mathbf{S}} \|\mathbf{P}\mathbf{S}\|_* \quad \text{s.t.} \quad \begin{cases} \mathbf{S} \in \mathcal{C}_{\mathcal{V}_K}, \\ \mathbf{S} \in \mathcal{C}_{L'}. \end{cases} \quad (19)$$

This Eq. (19) is equivalent to the following minimization problem by introducing the indicator functions for the sets  $\mathcal{C}_{\mathcal{V}_K}$  and  $\mathcal{C}_{L'}$ :

$$\min_{\mathbf{S}} \iota_{\mathcal{C}_{\mathcal{V}_K}}(\mathbf{S}) + \iota_{\mathcal{C}_{L'}}(\mathbf{S}) - \|\mathbf{P}\mathbf{S}\|_*. \quad (20)$$

Next, we address the non-convex combinatorial constraint  $\iota_{\mathcal{C}_{L'}}(\mathbf{S})$ . We replace this intractable indicator function with a DC penalty term that promotes sparsity among the rows corresponding to the set  $\mathcal{V}_U$ . Then, Eq. (20) is transformed into the following formulation:

$$\min_{\mathbf{S}} \iota_{\mathcal{C}_{\mathcal{V}_K}}(\mathbf{S}) + \lambda \left( \sum_{i \in \mathcal{V}_U} \|\mathbf{s}_{(i)}\|_2 - \Omega_{L'}(\mathbf{S}_{\mathcal{V}_U}) \right) - \|\mathbf{P}\mathbf{S}\|_*, \quad (21)$$

where  $\mathbf{S}_{\mathcal{V}_U}$  is the sub-matrix of  $\mathbf{S}$  with rows from  $\mathcal{V}_U$ ,  $\Omega_{L'}(\mathbf{X})$  is a function summing the  $\ell_2$  norms of the  $L'$  largest rows of  $\mathbf{X}$ , and  $\lambda > 0$  is a parameter.

Finally, by rearranging the terms to fit the DC structure and adding a regularization term  $\frac{\delta}{2} \|\mathbf{S}\|_F^2$  ( $\delta > 0$ ) to ensure the objective function is bounded below, we arrive at our final DC optimization problem:

$$\min_{\mathbf{S}} \left( \iota_{\mathcal{C}_{\mathcal{V}_K}}(\mathbf{S}) + \lambda \sum_{i \in \mathcal{V}_U} \|\mathbf{s}_{(i)}\|_2 + \frac{\delta}{2} \|\mathbf{S}\|_F^2 \right) - (\|\mathbf{P}\mathbf{S}\|_* + \lambda \Omega_{L'}(\mathbf{S}_{\mathcal{V}_U})). \quad (22)$$

Here, both the first and second parenthesized terms are proper lower semi-continuous convex functions, and the objective function is lower bounded.

### C. Optimization

The proposed problem (22) has a DC structure and can be solved efficiently using the GDPGDC algorithm. We map our problem to the general form in (10) by setting the components as follows:

$$f_1(\mathbf{X}) = 0, \quad (23)$$

$$f_2(\mathbf{X}) = \iota_{\mathcal{C}_{\mathcal{V}_K}}(\mathbf{X}) + \lambda \sum_{i \in \mathcal{V}_U} \|\mathbf{x}_{(i)}\|_2 + \frac{\delta}{2} \|\mathbf{X}\|_F^2, \quad (24)$$

$$h(\mathbf{Z}) = \|\mathbf{Z}_1\|_* + \lambda \Omega_{L'}(\mathbf{Z}_2), \quad (25)$$

$$\mathbf{Z} = \begin{bmatrix} \mathbf{Z}_1 \\ \mathbf{Z}_2 \end{bmatrix} = \mathbf{B}\mathbf{X}, \quad \mathbf{B} = \begin{bmatrix} \mathbf{P} \\ \mathbf{I}_{\mathcal{V}_U} \end{bmatrix}, \quad \mathbf{X} = \mathbf{S}, \quad (26)$$

where  $\mathbf{I}_{\mathcal{V}_U} \in \mathbb{R}^{|\mathcal{V}_U| \times N}$  is a selection matrix that extracts the rows corresponding to the undecided set  $\mathcal{V}_U$  from a matrix. The function  $f_2$  groups the non-contributive vertex constraint, the sparsity-inducing term for undecided vertices, and the regularization term. The function  $h$  corresponds to the convex terms we aim to maximize: the nuclear norm for the best possible recovery and the sum of the largest row norms to control the number of selected vertices.

The GDPGDC algorithm, summarized in Algorithm 1, involves two main steps that can be solved analytically. The first step (line 2 in Algorithm 1) requires computing  $\text{prox}_{\gamma_1 f_2}(\cdot)$ . Since  $f_2$  is separable row-wise, this can be computed for each row  $\mathbf{x}_{(i)}$  of a given matrix  $\mathbf{X}$  as:

$$\begin{aligned} [\text{prox}_{\gamma_1 f_2}(\mathbf{X})]_{(i)} &= \\ &\begin{cases} \mathbf{0}, & \text{if } i \in \mathcal{V}_K, \\ \frac{1}{1+\gamma_1\delta} \max\left(0, 1 - \frac{\gamma_1\lambda}{\|\mathbf{x}_{(i)}\|_2}\right) \mathbf{x}_{(i)}, & \text{if } i \in \mathcal{V}_U, \\ \frac{1}{1+\gamma_1\delta} \mathbf{x}_{(i)}, & \text{if } i \in \mathcal{V}_C. \end{cases} \end{aligned} \quad (27)$$

For the detail of this calculation, see Appendix A.

The second step (line 3) involves  $\text{prox}_{\gamma_2 h^*}(\cdot)$ , which is calculated via Moreau's identity (13) using  $\text{prox}_{\frac{1}{\gamma_2} h}(\cdot)$ . The computation of  $\text{prox}_{\gamma h}(\mathbf{Z})$  can be decomposed into two independent blocks as follows:

$$\text{prox}_{\gamma h}(\mathbf{Z}) = \begin{bmatrix} \text{prox}_{\gamma \|\cdot\|_*}(\mathbf{Z}_1) \\ \text{prox}_{\gamma \lambda \Omega_{L'}(\cdot)}(\mathbf{Z}_2) \end{bmatrix}. \quad (28)$$

---

### Algorithm 1 GDPGDC-based algorithm for solving (22)

---

**Input:**  $\mathbf{S}^{(0)}, \mathbf{Z}^{(0)}, \gamma_1^{(0)} > 0, \gamma_2^{(0)} > 0$   
1: **while** a stopping criterion is not met **do**  
2:    $\mathbf{S}^{(t+1)} \leftarrow \text{prox}_{\gamma_1^{(t)} f_2} \left( \mathbf{S}^{(t)} + \gamma_1^{(t)} \mathbf{B}^\top \mathbf{Z}^{(t)} \right)$ ;  
3:    $\mathbf{Z}^{(t+1)} \leftarrow \text{prox}_{\gamma_2^{(t)} h^*} \left( \mathbf{Z}^{(t)} + \gamma_2^{(t)} \mathbf{B} \mathbf{S}^{(t+1)} \right)$ ;  
4:    $t \leftarrow t + 1$ ;  
5: **end while**  
**Output:**  $\mathbf{S}^{(t)}$

---

The proximity operator for the first block,  $\text{prox}_{\gamma \|\cdot\|_*}(\mathbf{Z}_1)$ , is computed as follows:

$$\text{prox}_{\gamma \|\cdot\|_*}(\mathbf{Z}_1) = \mathbf{U}_{\mathbf{Z}_1} \mathcal{S}_\gamma(\boldsymbol{\Sigma}_{\mathbf{Z}_1}) \mathbf{V}_{\mathbf{Z}_1}^\top, \quad (29)$$

where  $\mathbf{U}_{\mathbf{Z}_1}$  and  $\mathbf{V}_{\mathbf{Z}_1}$  are the left and right singular vectors of  $\mathbf{Z}_1$ , respectively, and  $\mathcal{S}_\gamma(\cdot)$  is the soft-thresholding operator applied to the singular values, defined as:  $\mathcal{S}_\gamma(\sigma_i) = \max(\sigma_i - \gamma, 0)$ , and  $\mathcal{S}_\gamma(\boldsymbol{\Sigma}_{\mathbf{Z}_1})$  is a diagonal matrix with entries  $\mathcal{S}_\gamma(\sigma_i(\mathbf{Z}_1))$ .

The second block,  $\text{prox}_{\gamma \lambda \Omega_{L'}(\cdot)}(\mathbf{Z}_2)$ , is analytically computable through a two-stage process [43]. First, an optimal threshold is determined from the row  $\ell_2$  norms of  $\mathbf{Z}_2$ . Let  $z_i = \|\mathbf{Z}_2\|_{(i)}\|_2$  be the  $\ell_2$  norm of the  $i$ -th row of  $\mathbf{Z}_2$ , and let  $\mu_1 \geq \mu_2 \geq \dots$  be the sorted values of  $z_i$  in descending order. We find the largest index  $k^* \in \{1, \dots, L'\}$  such that

$$\mu_{k^*} > \frac{1}{k^*} \left( \sum_{j=1}^{k^*} \mu_j - \gamma \lambda \right). \quad (30)$$

Second, based on the outcome, each row  $[\mathbf{Z}_2]_{(i)}$  is updated. If such a  $k^*$  exists, the update is given by:

$$\begin{aligned} &[\text{prox}_{\gamma \lambda \Omega_{L'}(\cdot)}(\mathbf{Z}_2)]_{(i)} \\ &= \max \left( 0, 1 - \frac{\sum_{j=1}^{k^*} \mu_j - \gamma \lambda}{k^* \|\mathbf{Z}_2\|_{(i)}\|_2} \right) [\mathbf{Z}_2]_{(i)}. \end{aligned} \quad (31)$$

If no such  $k^*$  exists, the output is simply the input matrix, i.e.,  $\text{prox}_{\gamma \lambda \Omega_{L'}(\cdot)}(\mathbf{Z}_2) = \mathbf{Z}_2$ .

**Remark 1** (Convergence of the proposed algorithm). Since the objective function of Prob. (22) is bounded below and  $f_2$  and  $h$  are proper lower semi-continuous convex functions, the assumptions in Theorem 1 are satisfied. This ensures that the sequences  $\{\mathbf{S}^{(t)}\}_{t \in \mathbb{N}}$  and  $\{\mathbf{Z}^{(t)}\}_{t \in \mathbb{N}}$  generated by Algorithm 1 are bounded. Therefore, the sequence  $\{\mathbf{S}^{(t)}\}_{t \in \mathbb{N}}$  is guaranteed to converge to a critical point of Prob. (22).

## IV. Experiments and Results

We demonstrated the effectiveness of our method through sampling and recovering experiments across various types of graph signals. All experiments were conducted using MATLAB (R2024b) on a Windows 11 computer with Intel Core i9-14900KF 3.20-GHz processor, 32 GB of RAM, and NVIDIA GeForce RTX 4090. Our method was compared with the following graph signal sampling methods: SP [20], AVM [26], GSSS [33], and ScFGSS [37]. SP and AVM

are representative methods for sampling bandlimited graph signals. GSSS is a vertex-wise sampling method for sampling beyond bandlimited graph signals under arbitrary priors in the graph vertex domain. ScFGSS is a vertex-wise flexible sampling method for sampling beyond bandlimited graph signals under arbitrary priors in the graph vertex domain and controlling the number of sample-contributive vertices without constraints on sample-contributive or non sample-contributive vertices.

### A. Synthetic Data

#### 1) Setup

We generated random sensor graphs, which are implemented by  $k$  nearest neighbor graphs, whose vertices are randomly distributed in 2-D space  $[0, 1] \times [0, 1]$ , with consisting of  $N = 256$  vertices by using GSPBox [44]. The size of sampled signal was set as  $M = 32$ . The sampling and recovering framework is illustrated in Fig. 1.

We have generated the following types of graph signals for the  $i$ -th and the largest graph frequency,  $\lambda_i$  and  $\lambda_{\max}$ :

- SB prior: Periodic graph spectrum (PGS) [45] signals with the generator response of  $\mathbf{A}$ ,  $\hat{A}(\lambda_i) = \exp(-1.5\lambda_i/\lambda_{\max})$  and  $\mathbf{d}$  with  $d_i \sim \mathcal{N}(1, 1)$  for any  $i = 1, \dots, K$ , and  $K = 16$ ;
- SM prior: Gaussian Markov random field (GMRF) [46] with the power spectrum  $\hat{\Gamma}_{\mathbf{x}}(\lambda_i) = 0.1/(\lambda_i + 0.1)$  for any  $i = 1, \dots, N$ ;
- ST prior: GMRF with the power spectrum  $\hat{\Gamma}_{\mathbf{x}}(\lambda_i) = \exp\left(-((2\lambda_i - \lambda_{\max})/\sqrt{\lambda_{\max}})^2\right)$  for any  $i = 1, \dots, N$ .

For all graph types above, we also experimented with noisy sampled signals  $\mathbf{y} := \mathbf{c} + \boldsymbol{\eta}$ , where  $\boldsymbol{\eta} \in \mathbb{R}^M$  is generated as a zero-mean white Gaussian noise with its variance  $\sigma^2 = 0.1$ .

We set the desired upper limit of sample-contributive vertices  $L = 32$ , and the number of known sample-contributive vertices  $|\mathcal{V}_C|$  and the number of known non sample-contributive vertices  $|\mathcal{V}_K|$  as  $|\mathcal{V}_C| = |\mathcal{V}_K| = 16$ . We designed the sampling operator  $\mathbf{S}$  in the following three patterns:

- Design (i):  $\mathcal{V}_C$  is set to 16 vertices selected by the greedy algorithm proposed in [33], and  $\mathcal{V}_K$  is set to 16 randomly selected vertices from the remaining vertices not selected in the aforementioned 16 vertices.
- Design (ii):  $\mathcal{V}_C$  is set to 16 randomly selected vertices from the entire vertices, and  $\mathcal{V}_K$  is set to 16 randomly selected vertices from the remaining vertices.
- Design (iii):  $\mathcal{V}_K$  is set to 16 randomly selected vertices from the first 32 vertices selected by the greedy algorithm proposed in [33], and  $\mathcal{V}_C$  is set to 16 randomly selected vertices from the remaining vertices not selected in the aforementioned 32 vertices.

The parameters for the proposed method are summarized in Table 3, and  $\gamma_1^{(t)}, \gamma_2^{(t)}$  were decreased by 0.01% at each

TABLE 3. Parameters for the Proposed Method.

Prior	$\lambda$	$\delta$	$\gamma_1^{(0)}$	$\gamma_2^{(0)}$
Subspace (SB)	1.05	$10^{-1}$	$10^{-3}$	$10^{-5}$
Smoothness (SM)	5.1	$10^{-1}$	$10^{-2}$	$10^{-2}$
Stochastic (ST)	0.75	$10^{-6}$	$10^{-3}$	$10^{-5}$

iteration. For the existing methods, we used the parameters described in the respective papers.

We defined the initial value  $\mathbf{S}^{(0)}$  as a matrix with random Gaussian entries, and the stopping criterion in Algorithm 1 as  $\|\mathbf{S}^{(t+1)} - \mathbf{S}^{(t)}\|_F / \|\mathbf{S}^{(t)}\|_F \leq 10^{-5}$ . The parameter settings for the existing methods followed the descriptions in the respective papers, and a graph filter used in GSSS was set as an identity matrix.

For sampling graph signals under the smoothness prior, we used the spectral response  $F(\mathbf{A})$  of the smoothness operator  $\mathbf{F}$  following as  $F(\lambda_i) = \lambda_i/\lambda_{\max} + 0.1$ .

For the quantitative evaluations, we used MSE:  $\text{MSE} = \|\tilde{\mathbf{x}} - \mathbf{x}\|_2^2/N$ , where  $\tilde{\mathbf{x}}$  and  $\mathbf{x}$  are the recovered and original graph signals, respectively. As a note, smaller values of the MSE indicate better recovery accuracy.

#### 2) Results and Discussion

Table 4 represents the averaged MSEs in decibels between original graph signals and recovered graph signals generated by each method obtained from 20 independent runs for each graph signal type. Table 5 represents the average number of sample-contributive vertices by the sampling operators designed by the proposed method for 20 independent runs. Fig. 2 visualizes examples of the original and recovered graph signals. Fig. 3 visualizes the sampling operators designed by the proposed method for the PGS graph signal illustrated in Fig. 2.

The results shown in Table 4, comparing the results of SP and AVM, methods specialized for BL graph signals, with those of GSSS, ScFGSS, and the proposed method, methods applicable to beyond BL graph signals, the latter methods are superior in any cases. This shows the effectiveness of a sampling method for beyond BL graph signals based on the generalized sampling theory.

Furthermore, comparing the results of GSSS, which performs a vertex-wise sampling, with those of ScFGSS and the proposed method, which perform vertex-wise flexible sampling with and without the constraints on prior knowledge of vertices, respectively, in most cases, especially in cases with noise, ScFGSS and the proposed method achieved better results. This indicates the effectiveness of flexible sampling approaches. However, even among the proposed methods, the results of Design (ii) and (iii) are inferior to those of ScFGSS and Design (i) in some cases. This is due to the fact that the settings of known sample-contributive and non sample-contributive vertices are random or that important vertices may be excluded, respectively. In addition, in the noiseless case of the subspace prior, GSSS achieved the best result; however, GSSS, ScFGSS, and the proposed method

**TABLE 4. Average MSEs in Decibel of the Recoveries for 20 Independent Runs on each Method.**

Signal Prior	SP [20]	AVM [26]	GSSS [33]	ScFGSS [37]	Design (i)	Design (ii)	Design (iii)
SB (PGS)	-19.672	-18.474	<b>-612.924</b>	-604.539	-606.181	<u>-608.050</u>	-601.380
+ noise	-14.896	-13.730	-27.669	<b>-38.753</b>	<u>-37.838</u>	-22.354	-16.717
SM (GMRF)	-23.630	-6.125	-27.559	<b>-27.739</b>	<u>-27.679</u>	-27.395	-27.392
+ noise	-18.003	-4.600	-22.608	<u>-26.960</u>	<b>-27.374</b>	-26.428	-25.900
ST (GMRF)	-20.758	-9.036	-25.243	-26.235	<b>-26.705</b>	<u>-26.617</u>	-26.572
+ noise	-15.137	-6.158	-23.972	<b>-25.933</b>	<u>-25.553</u>	-25.373	-25.368

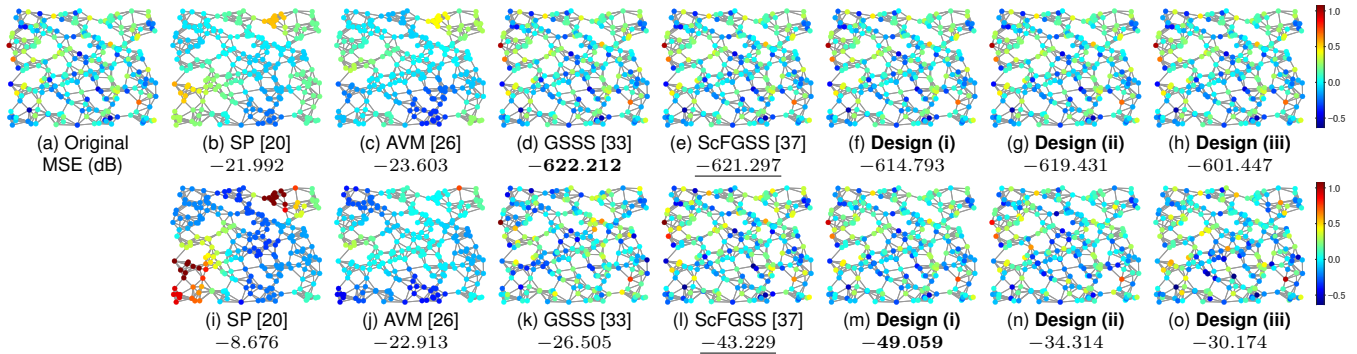


**FIGURE 2. An example of sampling and recovery experiment on a PGS graph signal on a random sensor graph ( $N = 256$ ,  $M = L = 32$ ). Fig. (a) shows the original PGS signal. Figs. (b)-(h) show the recovered signals from the noiseless sampled signals, and Figs. (i)-(o) show the recovered signals from the noisy sampled signals. The results in MSE are expressed in decibels, where smaller values indicate better recovery accuracy. The best and second best results in each case are in bold and underlined, respectively.**

**TABLE 5. Average Number of Sample-Contributive Vertices by the Proposed Method for 20 Independent Runs.**

Signal Prior	Design (i)	Design (ii)	Design (iii)
SB (PGS)	24.20	33.60	31.50
SM (GMRF)	30.75	31.10	31.00
ST (GMRF)	31.85	31.85	32.00

**TABLE 6. Parameters for the Proposed Method.**

Prior	$\lambda$	$\delta$	$\gamma_1^{(0)}$	$\gamma_2^{(0)}$
Smoothness (SM)	24.29	$10^{-6}$	$10^{-3}$	$10^{-5}$
Stochastic (ST)	6.03	$10^{-1}$	$10^{-3}$	$10^{-5}$

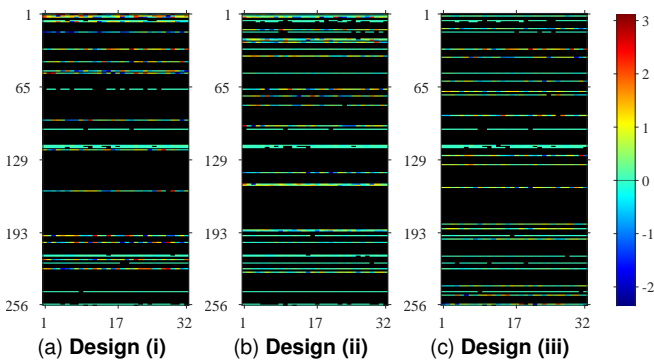


**FIGURE 3. Sampling operators designed by the proposed method for the graph signal in Fig. 2. Zero values are shown in black.**

all achieved very good results with MSEs exceeding  $-600$  dB ( $10^{-31}$ ).

The results of ScFGSS and Design (i) of the proposed method are almost equivalent in many cases. Here, in the proposed method, there are constraints on sample-contributive and non sample-contributive vertices, while in ScFGSS, there are no such constraints, allowing for a more flexible design of the sampling operator. In addition, in the proposed method,

the number of sample-contributive vertices is controlled by a penalty term in the objective function, making it difficult to strictly control the number that the number is less than 32 as shown in Table 5; however, in ScFGSS, this number is strictly controlled to be exactly 32. The fact that the proposed method can achieve results equivalent to those of ScFGSS under these conditions demonstrates the effectiveness of the proposed method that can handle constraints on sample-contributive and non sample-contributive vertices.

In Fig. 2, an example of the recovery results is visualized, which also shows that high accurate sampling and recovery is achieved by the proposed method. In Fig. 3, an example of the sampling operators designed by the proposed method is shown, which also shows that the sampling operators designed by the proposed method can control the number of sample-contributive vertices.

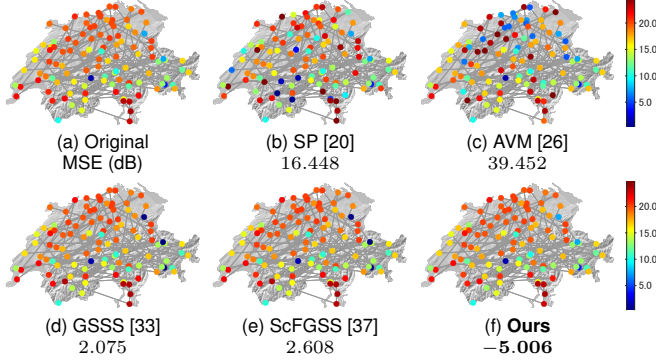
## B. Real-World Data

### 1) Setup

We used a dataset of monthly average temperatures from 2015 to 2024 at  $N = 110$  locations in Switzerland [47]. The data was divided into two periods. Data from 2015 to 2019 was used to construct the graph via a graph learning method [5] for the smoothness prior and to estimate the

**TABLE 7. Average MSEs in Decibel of the Recoveries for Monthly Average Temperature at 110 Spots in Switzerland.**

Prior	SP	AVM	GSSS	ScFGSS	Ours
SM	12.307	29.245	2.884	2.577	<b>-4.960</b>
+ noise	12.477	29.450	4.143	5.478	<b>1.997</b>
ST	—	—	-19.953	-20.872	<b>-21.880</b>
+ noise	—	—	-18.635	-20.702	<b>-21.819</b>

**FIGURE 4. Signal recovery experiments for the average temperature of Switzerland in July with assuming the smoothness prior ( $N = 110$ ,  $M = L = 28$ ). Fig. (a) shows the original temperature. Figs. (b)-(f) show the sampled and recovered temperatures. The best result is in bold.**

signal covariance matrix [48] for the stochastic prior. The data from 2020 to 2024 served as the graph signals for the sampling and recovery experiments. The overall sampling and recovery framework is illustrated in Fig. 1.

For each graph signal, the size of sampled signal was set to  $M = 28$ . We also conducted experiments where zero-mean white Gaussian noise with a variance of  $\sigma^2 = 0.1$  was added to the sampled signals. For experiments assuming a smoothness prior, the smoothness operator  $\mathbf{F}$  was defined by its spectral response  $F(\lambda_i) = \lambda_i / \lambda_{\max} + 0.01$ .

For the proposed method, we set the desired upper limit of sample-contributive vertices to  $L = 28$ . The sets of known sample-contributive and non sample-contributive vertices were defined as  $|\mathcal{V}_C| = |\mathcal{V}_K| = 14$ . We employed the same vertex selection strategy as Design (i) described in the synthetic data experiments. The other parameters for our method are summarized in Table 6, with  $\gamma_1^{(t)}, \gamma_2^{(t)}$  being decreased by 0.01% at each iteration.

The performance of our method was compared against the same existing methods from the synthetic data experiments, using the average MSE as the evaluation metric.

## 2) Results

Table 7 shows the average MSEs in decibels between original and recovered graph signals. The methods proposed in SP and AVM do not consider the difference of the priors, thus their results are only listed in the smoothness prior row. Fig. 4 visualizes examples of the original and recovered graph signals of the average temperature across Switzerland in July from 2020 to 2024. Both results demonstrate that the proposed method outperforms existing methods.

## V. Conclusion

We proposed a method to design a sampling operator to achieve vertex-wise flexible sampling for beyond bandlimited graph signals. The design was formulated as an optimization problem with a rank constraint to achieve the best possible recovery based on the generalized sampling theory, a constraint to control the number of sample-contributive vertices, and constraint to handle prior knowledge of sets of sample-contributive and non sample-contributive vertices. The problem was transformed into a DC optimization problem by relaxing the rank and controlling the number of sample-contributive vertices constraints using a nuclear norm and a DC penalty term, respectively. To solve it, we developed a solver based on the GDPGDC algorithm, which guarantees convergence to a critical point. Experiments demonstrated the effectiveness of our method.

## Appendix

### A. The Calculation of Eq. (27)

Since  $f_2$  described in Eq. (24) is separable row-wise, each row of  $\text{prox}_{\gamma f_2}(\mathbf{X})$  can be represented as follows:

$$\begin{aligned} & [\text{prox}_{\gamma f_2}(\mathbf{X})]_{(i)} \\ &= \underset{\mathbf{y}_{(i)}}{\text{argmin}} \left\{ \alpha \iota_0(\mathbf{y}_{(i)}) + \beta \lambda \|\mathbf{y}_{(i)}\|_2 + \frac{\delta}{2} \|\mathbf{y}_{(i)}\|_F^2 \right. \\ & \quad \left. + \frac{1}{2\gamma} \|\mathbf{x}_{(i)} - \mathbf{y}_{(i)}\|_F^2 \right\}, \quad (32) \end{aligned}$$

where  $\alpha = 1$  if  $i \in \mathcal{V}_K$  and  $\alpha = 0$  otherwise, and  $\beta = 1$  if  $i \in \mathcal{V}_U$  and  $\beta = 0$  otherwise. We consider the following cases of which set the vertex  $i$  belongs to.

- $i \in \mathcal{V}_K$ : The indicator function  $\iota_0(\mathbf{y}_{(i)})$  enforces

$$[\text{prox}_{\gamma f_2}(\mathbf{X})]_{(i)} = \mathbf{0}. \quad (33)$$

- $i \in \mathcal{V}_U$ : Eq. (32) can be written as

$$\begin{aligned} & [\text{prox}_{\gamma f_2}(\mathbf{X})]_{(i)} \\ &= \underset{\mathbf{y}_{(i)}}{\text{argmin}} \left\{ \lambda \|\mathbf{y}_{(i)}\|_2 + \frac{\delta}{2} \|\mathbf{y}_{(i)}\|_F^2 + \frac{1}{2\gamma} \|\mathbf{x}_{(i)} - \mathbf{y}_{(i)}\|_F^2 \right\}. \quad (34) \end{aligned}$$

This is the proximity operator of the sum of the  $\ell_2$  norm and the squared  $\ell_2$  norm, and its solution is given by

$$[\text{prox}_{\gamma f_2}(\mathbf{X})]_{(i)} = \frac{1}{1 + \gamma\delta} \max \left\{ 0, 1 - \frac{\gamma\lambda}{\|\mathbf{x}_{(i)}\|_2} \right\} \mathbf{x}_{(i)}. \quad (35)$$

- $i \in \mathcal{V}_C$ : Eq. (32) can be written as

$$\begin{aligned} & [\text{prox}_{\gamma f_2}(\mathbf{X})]_{(i)} \\ &= \underset{\mathbf{y}_{(i)}}{\text{argmin}} \left\{ \frac{\delta}{2} \|\mathbf{y}_{(i)}\|_F^2 + \frac{1}{2\gamma} \|\mathbf{x}_{(i)} - \mathbf{y}_{(i)}\|_F^2 \right\}. \quad (36) \end{aligned}$$

This is the proximity operator of the squared  $\ell_2$  norm, and its solution is given by

$$[\text{prox}_{\gamma f_2}(\mathbf{X})]_{(i)} = \frac{1}{1 + \gamma\delta} \mathbf{x}_{(i)}. \quad (37)$$

Therefore, Eq. (27) is obtained by Eqs. (33), (35), and (37).

## REFERENCES

- [1] S. K. Narang and A. Ortega, "Perfect reconstruction two-channel wavelet filter banks for graph structured data," *IEEE Trans. Signal Process.*, vol. 60, no. 6, pp. 2786–2799, 2012.
- [2] A. Agaskar and Y. M. Lu, "A spectral graph uncertainty principle," *IEEE Trans. Inf. Theory*, vol. 59, no. 7, pp. 4338–4356, 2013.
- [3] D. I. Shuman, M. J. Faraji, and P. Vandergheynst, "A multiscale pyramid transform for graph signals," *IEEE Trans. Signal Process.*, vol. 64, no. 8, pp. 2119–2134, 2015.
- [4] Y. Tanaka and Y. C. Eldar, "Generalized sampling on graphs with subspace and smoothness priors," *IEEE Trans. Signal Process.*, vol. 68, pp. 2272–2286, 2020.
- [5] X. Dong, D. Thanou, P. Frossard, and P. Vandergheynst, "Learning Laplacian matrix in smooth graph signal representations," *IEEE Trans. Signal Process.*, vol. 64, no. 23, pp. 6160–6173, 2016.
- [6] H. E. Egilmez, E. Pavez, and A. Ortega, "Graph learning from filtered signals: Graph system and diffusion kernel identification," *IEEE Trans. Signal Inf. Process. Netw.*, vol. 5, no. 2, pp. 360–374, 2018.
- [7] Y. Liu, L. Yang, K. You, W. Guo, and W. Wang, "Graph learning based on spatiotemporal smoothness for time-varying graph signal," *IEEE Access*, vol. 7, pp. 62372–62386, 2019.
- [8] S. Ono, I. Yamada, and I. Kumazawa, "Total generalized variation for graph signals," in *Proc. IEEE Int. Conf. Acoust., Speech, Signal Process. (ICASSP)*, 2015, pp. 5456–5460.
- [9] M. Onuki, S. Ono, M. Yamagishi, and Y. Tanaka, "Graph signal denoising via trilateral filter on graph spectral domain," *IEEE Trans. Signal Inf. Process. Netw.*, vol. 2, no. 2, pp. 137–148, 2016.
- [10] Peter Berger, Gabor Hannak, and Gerald Matz, "Graph signal recovery via primal-dual algorithms for total variation minimization," *IEEE J. Sel. Top. Signal Process.*, vol. 11, no. 6, pp. 842–855, 2017.
- [11] M. Nagahama, K. Yamada, Y. Tanaka, S. H. Chan, and Y. C. Eldar, "Graph signal restoration using nested deep algorithm unrolling," *IEEE Trans. Signal Process.*, vol. 70, pp. 3296–3311, 2022.
- [12] E. Yamagata, K. Naganuma, and S. Ono, "Robust time-varying graph signal recovery for dynamic physical sensor network data," *IEEE Trans. Signal Inf. Process. Netw.*, 2025.
- [13] G. Cheung, E. Magli, Y. Tanaka, and M. K. Ng, "Graph spectral image processing," *Proc. IEEE*, vol. 106, no. 5, pp. 907–930, 2018.
- [14] A. Hasanzadeh, X. Liu, N. Duffield, and K. R. Narayanan, "Piecewise stationary modeling of random processes over graphs with an application to traffic prediction," in *Proc. IEEE Int. Conf. Big Data*, 2019, pp. 3779–3788.
- [15] M. Zare, M. S. Helfroush, and K. Kazemi, "Fusing hyperspectral and multispectral images using smooth graph signal modelling," *Int. J. Remote Sens.*, vol. 41, no. 22, pp. 8610–8630, 2020.
- [16] S. Takemoto, K. Naganuma, and S. Ono, "Graph spatio-spectral total variation model for hyperspectral image denoising," *IEEE Trans. Geosci. Remote Sens.*, vol. 19, pp. 1–5, 2022.
- [17] Y. Tanaka, Y. C. Eldar, A. Ortega, and G. Cheung, "Sampling signals on graphs: From theory to applications," *IEEE Signal Process. Mag.*, vol. 37, no. 6, pp. 14–30, 2020.
- [18] S. Chen, R. Varma, A. Sandryhaila, and J. Kovačević, "Discrete signal processing on graphs: Sampling theory," *IEEE Trans. Signal Process.*, vol. 63, no. 24, pp. 6510–6523, 2015.
- [19] A. G. Marques, S. Segarra, G. Leus, and A. Ribeiro, "Sampling of graph signals with successive local aggregations," *IEEE Trans. Signal Process.*, vol. 64, no. 7, pp. 1832–1843, 2015.
- [20] A. Anis, A. Gadde, and A. Ortega, "Efficient sampling set selection for bandlimited graph signals using graph spectral proxies," *IEEE Trans. Signal Process.*, vol. 64, no. 14, pp. 3775–3789, 2016.
- [21] M. Tsitsvero, S. Barbarossa, and P. Di Lorenzo, "Signals on graphs: Uncertainty principle and sampling," *IEEE Trans. Signal Process.*, vol. 64, no. 18, pp. 4845–4860, 2016.
- [22] D. Valsesia, G. Fracastoro, and E. Magli, "Sampling of graph signals via randomized local aggregations," *IEEE Trans. Signal Inf. Process. Netw.*, vol. 5, no. 2, pp. 348–359, 2018.
- [23] Y. Tanaka, "Spectral domain sampling of graph signals," *IEEE Trans. Signal Process.*, vol. 66, no. 14, pp. 3752–3767, 2018.
- [24] G. Puy, N. Tremblay, R. Gribonval, and P. Vandergheynst, "Random sampling of bandlimited signals on graphs," *Appl. Comput. Harmon. Anal.*, vol. 44, no. 2, pp. 446–475, 2018.
- [25] Y. Bai, F. Wang, G. Cheung, Y. Nakatsukasa, and W. Gao, "Fast graph sampling set selection using gershgorin disc alignment," *IEEE Trans. Signal Process.*, vol. 68, pp. 2419–2434, 2020.
- [26] A. Jayawant and A. Ortega, "Practical graph signal sampling with log-linear size scaling," *Signal Process.*, vol. 194, pp. 108436, 2022.
- [27] J. Li and B. Cai, "Sensor placement method for water distribution networks based on sampling of non-bandlimited graph signals," *Digital Signal Processing*, vol. 156, pp. 104809, 2025.
- [28] Y. C. Eldar and T. Michaeli, "Beyond bandlimited sampling," *IEEE Signal Process. Mag.*, vol. 26, no. 3, pp. 48–68, 2009.
- [29] Y. C. Eldar, *Sampling theory: Beyond bandlimited systems*, Cambridge University Press, 2015.
- [30] S. P. Chepuri, Y. C. Eldar, and G. Leus, "Graph sampling with and without input priors," in *Proc. IEEE Int. Conf. Acoust., Speech, Signal Process. (ICASSP)*, 2018, pp. 4564–4568.
- [31] J. Hara, Y. Tanaka, and Y. C. Eldar, "Generalized graph spectral sampling with stochastic priors," in *Proc. IEEE Int. Conf. Acoust., Speech, Signal Process. (ICASSP)*, 2020, pp. 5680–5684.
- [32] J. Hara, K. Yamada, S. Ono, and Y. Tanaka, "Design of graph signal sampling matrices for arbitrary signal subspaces," in *Proc. IEEE Int. Conf. Acoust., Speech, Signal Process. (ICASSP)*, 2021, pp. 5275–5279.
- [33] J. Hara and Y. Tanaka, "Sampling set selection for graph signals under arbitrary signal priors," in *Proc. IEEE Int. Conf. Acoust., Speech, Signal Process. (ICASSP)*, 2022, pp. 5732–5736.
- [34] J. Hara, Y. Tanaka, and Y. C. Eldar, "Graph signal sampling under stochastic priors," *IEEE Trans. Signal Process.*, vol. 71, pp. 1421–1434, 2023.
- [35] K. Yamashita, K. Naganuma, and S. Ono, "Generalized graph signal sampling under subspace priors by difference-of-convex minimization," in *Proc. Asia-Pac. Signal Inf. Process. Assoc. Annu. Summit Conf. (APSIPA ASC)*, 2024, pp. 1–6.
- [36] K. Yamashita, K. Naganuma, and S. Ono, "Generalized graph signal sampling by difference-of-convex optimization," *arXiv*, 2025, [Online]. Available: <https://arxiv.org/abs/2306.14634>.
- [37] K. Yamashita, K. Naganuma, and S. Ono, "Controlling the number of sample-contributive vertices in generalized sampling of graph signals," in *Proc. IEEE Int. Conf. Acoust., Speech, Signal Process. (ICASSP)*, 2025, pp. 1–5.
- [38] K. Naganuma and S. Ono, "Hyperspectral unmixing with row-sparsity enhancement: A difference-of-convex approach," in *Proc. Asia-Pac. Signal Inf. Process. Assoc. Annu. Summit Conf. (APSIPA ASC)*, 2024, pp. 1–5.
- [39] K. Sato, K. Naganuma, and S. Ono, "Enhancing hyperspectral anomaly detection by difference-of-convex sparse anomaly modeling," in *Proc. IEEE Int. Conf. Acoust., Speech, Signal Process. (ICASSP)*, 2024, pp. 9921–9925.
- [40] S. Banert and R. I. Boț, "A general double-proximal gradient algorithm for dc programming," *Math. Program.*, vol. 178, no. 1-2, pp. 301–326, 2019.
- [41] H. H. Bauschke and P. L. Combettes, *Correction to: convex analysis and monotone operator theory in Hilbert spaces*, Springer, 2017.
- [42] M. Fazel, *Matrix rank minimization with applications*, Ph.D. thesis, PhD thesis, Stanford University, 2002.
- [43] D. Brzyski, A. Gossmann, W. Su, and M. Bogdan, "Group slope-adaptive selection of groups of predictors," *J. Am. Stat. Assoc.*, vol. 114, no. 525, pp. 419–433, 2019.
- [44] N. Perraudin, J. Paratte, D. Shuman, L. Martin, V. Kalofolias, P. Vandergheynst, and D. K. Hammond, "GSPBOX: A toolbox for signal processing on graphs," *arXiv*, 2014, [Online]. Available: <https://arxiv.org/abs/1408.5781>.
- [45] S. Chen, R. Varma, A. Singh, and J. Kovačević, "Representations of piecewise smooth signals on graphs," in *Proc. IEEE Int. Conf. Acoust., Speech, Signal Process. (ICASSP)*, 2016, pp. 6370–6374.
- [46] A. Gadde and A. Ortega, "A probabilistic interpretation of sampling theory of graph signals," in *Proc. IEEE Int. Conf. Acoust., Speech, Signal Process. (ICASSP)*, 2015, pp. 3257–3261.
- [47] Federal Office of Meteorology and Climatology MeteoSwiss, "Homogeneous climate station data," [https://opendatadocs.meteoswiss.ch/c-climate-data/c1-climate-stations\\_homogeneous](https://opendatadocs.meteoswiss.ch/c-climate-data/c1-climate-stations_homogeneous), 2025.
- [48] Nathanaël Perraudin and Pierre Vandergheynst, "Stationary signal processing on graphs," *IEEE Trans. Signal Process.*, vol. 65, no. 13, pp. 3462–3477, 2017.